SCIENTIFIC REPORTS
nature research

OPEN

Metabolomics Deciphered Metabolic Reprogramming Required for Biofilm Formation

Received: 4 April 2019
Accepted: 27 August 2019
Published online: 11 September 2019

Haitao Lu[1], Yumei Que[2], Xia Wu[2], Tianbing Guan[2] & Hao Guo[2]

Biofilm formation plays a key role in many bacteria causing infections, which mostly accounts for high-frequency infectious recurrence and antibiotics resistance. In this study, we sought to compare modified metabolism of biofilm and planktonic populations with UTI89, a predominant agent of urinary tract infection, by combining mass spectrometry based untargeted and targeted metabolomics methods, as well as cytological visualization, which enable us to identify the driven metabolites and associated metabolic pathways underlying biofilm formation. Surprisingly, our finding revealed distinct differences in both phenotypic morphology and metabolism between two patterns. Furthermore, we identified and characterized 38 differential metabolites and associated three metabolic pathways involving glycerolipid metabolism, amino acid metabolism and carbohydrate metabolism that were altered mostly during biofilm formation. This discovery in metabolic phenotyping permitted biofilm formation shall provide us a novel insight into the dissociation of biofilm, which enable to develop novel biofilm based treatments against pathogen causing infections, with lower antibiotic resistance.

Bacterial biofilms are fundamentally structured in a manner of a self-produced matrix of extracellular polymeric substance (EPS) with the extracellular DNAs, proteins and polysaccharides[1]. Biofilm formation drives the bacterial cells to persist survival and prolong their life-span, which has been observed to play a key role in many human infections with high-frequency antibiotic resistance[2]. Urinary Tract Infection (UTI) is a common, high-recurrence or even life-threaten infectious disease, which is mostly caused by uropathogenic *Escherichia coli* (UPEC). UPEC prefers to form biofilm and trigger the infections recurrently, thereby leading to uneasily eradicate UPEC strains by the treatment of antibiotics against UTI[1,3,4]. Basically, biofilm formations of bacteria have distinct stages involving attachment, micro colony formation and maturation, which are almost agreeable among different bacterial species. However, it still remains unclear if small-molecule metabolites and associated metabolism were required for biofilm formation and degradation. Our previous work verified that modified metabolism was observed to closely associate with the virulence expression of UPEC strains so as to promote the progression of UTIs, herein, reprogrammed metabolism might be the key factor for biofilm formation in terms of such structure directly contributes to high-pathogenicity and recurrence of UPEC strains during causing infections. Pellicle is a classical growth-mode of biofilm *in in vitro*, which is formed at the air-liquid interface without anchoring themselves to any solid surfaces[1,5]. UTI89 strain is a clinical UPEC strain that was originally isolated from the bladder of a woman with UTI, this stain is capable of forming a floating pellicle-biofilm in YESCA medium. To better understand the molecular phenotype of biofilm formation triggered by UPEC strain from a metabolic perspective, we aimed at investigate the biofilm formation by integrating staining assay, cytological observation with metabolomics method (Fig. 1A).

Materials and Methods

Reagents, bacterial strains and culture process. UTI89 was firstly incubated with LB broth (Miller's LB) (BD, Franklin Lakes, USA). The biofilm formation culture was facilitated statically in YESCA medium (1% Calamine Acids and 0.12% yeast extract) in 96-well plastic plates for Congo red and crystal violet for staining, as well as conical flask for metabolite enrichment and extraction. Briefly, one colony UTI89 strain was incubated with 7 ml LB broth for 5 hours on a shaker, and then the bacterial cells were diluted 100-fold into fresh YESCA

[1]Key Laboratory of Systems Biomedicine (Ministry of Education), Shanghai Center for Systems Biomedicine, Shanghai Jiao Tong University, Shanghai, 200240, China. [2]School of Pharmaceutical Sciences, Chongqing University, Chongqing, 401331, China. Haitao Lu and Yumei Que contributed equally. Correspondence and requests for materials should be addressed to H.L. (email: Haitao.lu@sjtu.edu.cn)

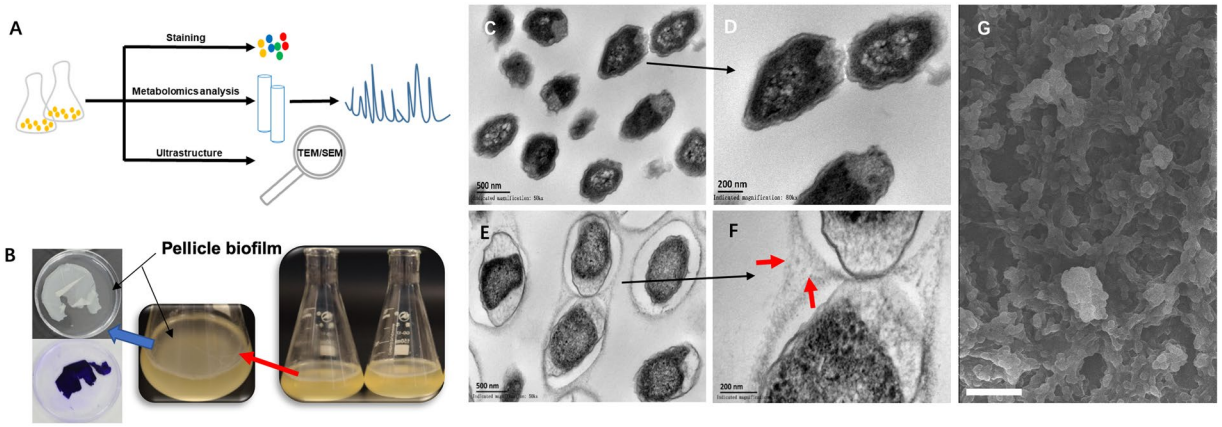

Figure 1. Combinational strategy characterized biofilm phenotype of UPEC UTI89 by integrating metabolomics method (**A**), staining assay (**B**) with cytological observation (**C**–**G**).

medium, then incubated at 30° for 96 hours statistically to trigger biofilm formation. The Congo red concentration was diluted in YESCA medium at 50 ug/ml. All the reference compounds for targeted metabolite assay were purchased from Sigma Company (Sigma, St. Louis, USA)

Crystal violet staining assay. Biofilm formation was quantified by crystal violet staining assay. Biofilm was initiated as previous described. The mature biofilm was washed with PBS for 3 times and then fixed biofilm with methanol for 15 minutes. After the methanol volatilized, 100 ul 1% crystal violet was added to the biofilm for 20 minutes. The dye wells with crystal violet were washed with PBS for 5 times. Bound crystal violet was solubilized with 100 ul 33% acetic acid for 30 minutes whilst shaking slowly. ODS value was measured via microplate reader at 570 nm. Statistical significance was determined by 2-tailed Student's T-test with a threshold $p\text{-value} < 0.05$

CFU assay. Each biofilm-sample was completely dispersed by manual-homogenizer in PBS for 20 times with the same physical pressure. The biofilm suspensions and planktonic cells were used to measure the CFU value. The following steps are recorded in reference[3]

SEM assay. Mature biofilm and the planktonic cells were fixed with 2.5% glutaraldehyde for more than 3 hours. Next, they were washed for three times with PBS, and then the specimen was first to be dehydrated by gradient-concentration ethanol (30%, 50%, 70%, 80%, 90% and 100%) for 5 minutes at each step. After that, the specimen was dehydrated again by the gradient-concentration tertiary butanol (70%, 90%, 95% and 100%). At last, the dehydrated specimen was coated with gold-palladium and observed in SEM (HITACHI S-3400N).

TEM assay. Mature biofilm and the planktonic cells were fixed with 2.5% glutaraldehyde for more than 3 hours. All the samples were embedded in 2% low-melt agarose, washed with PBS, and then fixed in 1% osmium tetroxide in cacodylate buffer for 1 hour. After that, the bacterial cells were post-fixed with osmium tetroxide, dehydrated in gradient- concentration ethanol and embedded subsequently in Epon 812. Specimens were sectioned with a diamond knife into 95 nm and they were finally analyzed using a transmission electron microscope S-3400N.

Metabolite extraction. Biofilm samples were isolated from 50 ml of culture solution, and the supernatants in the culture medium were spun down at 3500 rpm for 10 minutes to harvest the planktonic cells. Firstly, each biofilm was clean with PBS for 3 times, and added 2 ml the ice-cold methanol to mix by homogenizer for 2 minutes, all procedures were repeated for 3 times, but the samples were frozen and thawed within liquid nitrogen during the process. Secondly, the samples were centrifuged under12000 rpm at 4° for 10 minutes. The supernatants were mixed with 800 ul of ice-cold acetonitrile for 15 minutes before lyophilization. The dried samples were stored in −80° for GC-MS and LC-MS assay.

Sample derivation for GC/MS based metabolome assay. The lyophilized samples were resuspended in 40 ul of methoxyamine hydrochloride in pyridine (20 mg/ml) and completely mixed for 90 minutes at 30 °C. N-Methyl-N-(trimethylsilyl) trifluoroacetamide (MSTFA) (90 ul) was added to each sample, then mixed further for 30 minutes at 37 °C, and they were undergoing vortex before incubation. The derivative samples were centrifuged at 12000 rpm for 10 minutes and then transferred into a 2 ml GC vial and tightly capped for metabolome assay.

Data acquisition and analysis of GC/MS based metabolome assay. Metabolome assay was carried out on an Agilent 7890–5975 C GC/MS system using helium as the carrier gas at a constant flow. A total of 1 ul of sample was injected into a 50 m × 250 μm × 0.25 μm DB5-MS column using split less injection. The injector temperature was at 275 °C. Front-Pressure, average speed, flow rate was set at 22.468 psi, 34.908 cm/sec and 1.5 mL/minutes, respectively. The GC/MS data was firstly transformed to a digital data using XCMS online database and

then identified the metabolites by combining AMDIS software and associated database, which based on their retention index (RI) values along with the corresponding mass spectra. The identified metabolites were listed in a data-matrix file that was incorporated with metabolite ID, sample ID and the abundance of each metabolites, it was used for further pattern-recognition and statistical analyses.

Data acquisition and analysis of LC/MS based metabolome assay. Lyophilized samples were resuspended in 100 ul water and was injected to a UFLC-MS/MS system (AB SCIEX API 3200 TQ MS System; UFLC-SHIMADZU, 20AD) equipped with an ESI source in both negative and positive ion-modes with an electrospray ionization voltage of 5500 V for positive mode and 4500 V for negative mode, nebulizer gas (air), turbo gas (air), curtain gas (nitrogen) setting at 50, 50 and 25 psi respectively. Chromatographic separation was carried out on a Waters XSelect HSS T3 column (2.1 * 100 mm, 3.5 um) with a gradient program as follows: 5–95% Acetonitrile (Mobile Phase-B) for 50 minutes at a flow rate of 0.4 ml/minute. The column temperature was maintained at 40 °C, Mobile-Phase-A: 0.1% formic acid in water and Mobile Phase-B: 0.1% formic acid in acetonitrile. AB SCIEX Analyst software was used for data acquisition and preprocessing. The targeted MRM method was developed based on the acquired reference compounds, which assisted in targeted profiling the known compounds of interest from the known metabolic pathways.

Statistical analysis. The data matrix was transferred to MetaboAnalyst 3.0 version online to engage in multivariate statistical analysis including unsupervised principal component analysis (PCA), partial least squares discriminant analysis (PLS- DA) and heat-map overview. The loading plot (VIP plot) was used to discover and identify the differential metabolites, as well as the score plot was adopted to facilitate group classification. This brief method was referred to the publication[3].

Results and Discussion

Morphological observation verified successful development of biofilm model. Since notable morphological shifts of biofilm, pellicle and planktonic population were revealed in previous study[1]. We were first to confirm whether biofilm pellicle model was successful or not in our study (Fig. 1B), we employed the cytological method including Crystal Violet Staining, TEM (transmission electron microscope) and SEM (scanning electron microscope), to investigate the intricate-structure phenotype of biofilm formation, as it was expectedly found that pellicle biofilm have an organized and complex extracellular matrix-structure that encased individual, and spatially segregated bacterial-subpopulations (Fig. 1E,F), but such phenotype disappeared in the relevant planktonic-subpopulation (Fig. 1C,D). This result was completely consistent with previous study[1]. The imaging assay surely confirmed the biofilm pellicle model was successfully established in this study. In addition, staining technologies such as crystal violet and congo red were used to quantitatively assess the biofilm formation that was also significantly different from the planktonic population (Fig. S1). Those phenotypic observations may suggest us there is modified metabolism in two conditions.

Distinctly metabolic modifications were observed in both biofilm formation and associated planktonic-population. Metabolomics is an systems-biology driven omics method that was designed to global profiling all the small-molecule metabolites, whose level changes are capable of capturing and snapshotting different biological events and processes in cells with a diverse biological contexts[6,7]. To investigate reprogrammed-metabolism underlying biofilm formation, we explored one combinational strategy with untargeted and targeted metabolomics for deciphering the distinct metabolism that was critical for biofilm formation. Metabolome assay revealed that distinctly metabolic reprogramming during biofilm formation, which is significantly different from that in planktonic population (Fig. 2). From the score plot resulted from PLS-DA analysis of metabolome data harvested by LC/MS/MS system (Fig. 2A), we can see principal component 1 (PC-1) accounted for 31.3% of the variance, with PC-2 explaining 34%. The score plot by GC/MS based metabolome assay (Fig. 2B) indicated, principal component 1 (PC1) explained 58.9% of variance, with PC2 of 18.4%, which exhibit the greatest difference predominantly along the PC-1 analysis. Global metabolome result was also illustrated in Fig. 2C. Those results revealed remarkable metabolic-differentiation between biofilm formation and planktonic-subpopulation, while bacterial cells were switched to form biofilm, they could secret the extracellular polymeric substance (EPS), which can be used to protect biofilm to defense environment insults and difficult to dissolution. Although our TEM images only recognize the denser layer of fibers[1] (highlighted in red in Fig. 1E,F) surrounding bacteria in biofilm pellicle mode, many other components (eDNA, proteins and polysaccharides, *etc*) present in EPS structure[5–7] which were disappeared in planktonic population. We deduced that microbes are capable of sensing the density of microenvironment as well as releasing the signal to change the gene expression and further yielding the influence upon bacterial metabolism. Consequently, reprogrammed-metabolism would have feedback to the modification with morphological features of the biofilm. In addition, the data also suggested that there was a mechanistic association between biofilm metabolism and its' morphological feature.

Metabolic reprogramming triggered biofilm formation. Metabolic reprogramming is supposed to be the key driven-factor for biofilm formation even though such organism was structured by the involvements of multiple-layers molecules. We firstly demonstrated obvious modifications in both of small-molecule metabolism and morphological feature between biofilm and planktonic cells, however the profoundly metabolic mechanism remains largely unexplored. Here, we further combined the open-source databases with local database to identify the pivotal metabolites and associated metabolic pathways that have capacity to drive the biofilm formation while compared to planktonic cells. Unexpectedly, we successfully identified 38 differential metabolites, including amino acids, carbohydrates, organic acids, glycerol-derived, polyamine and uridine between biofilm pellicle and planktonic cell (Table S1). It was an amazing discovery as glycerol-derived metabolites (2-Phosphoglyceric acid, Glycerol 3-phosphate and D-Glyceraldehyde 3-phosphate) were significantly up-regulated during biofilm

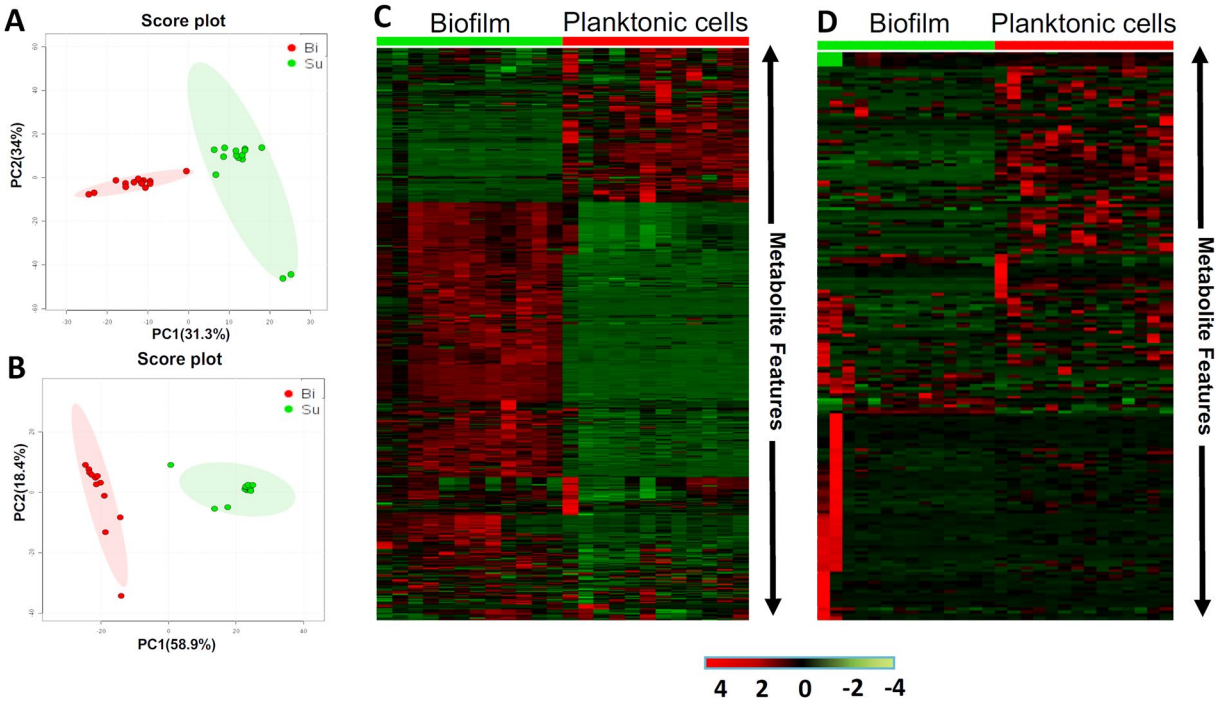

Figure 2. Metabolome assay revealed distinctly modified metabolism between biofilm and planktonic population. (**A**) Score plot resulted from unsupervised PCA analysis of LC/MS based metabolomics data. (**B**) Score plot resulted from unsupervised PCA analysis of GC/MS based metabolomics data. (**C**) Heatmap overviews of global metabolome data with upper one by LC/MS and bottom one by GC/MS. SU: planktonic cells; Bi: Biofilm.

formation while the glycerol was decreased considerably. Similarly, we also found that the levels of carbohydrates were enhanced clearly except that the levels of D-Maltose and D-Glucose were decreased in biofilm formation in relevant to that in planktonic cells. The level changes of other differential metabolites in both modes were showed in Table S1 and Fig. 3. Next, to home those differential metabolites to their metabolic pathways, we subjected them to metaboanalyst online to annotate associated metabolic pathways (Fig. 4). What metabolism we expected that were mostly reprogrammed that involved glycolipid metabolism, amino acid metabolism and carbohydrate metabolism, which were observed to markedly drive biofilm formation as most of differential metabolites were up-regulated accordingly (highlighted in blue in Fig. 4).

It was reported that proteins and carbohydrates were the main components of biofilm formation[2]. Several amino acids were documented to account for biofilm detachment and maturation[8–11]. In addition, the mixture of D-Amino acids would lead to the biofilm desperation with *Bacillus subtilis* and further break down the biofilm by YqxM protein which regulated the amyloid fibers anchoring or off-anchoring to the host cells[10]. However, our results only found the levels of many L-amino acids rather than D- amino acids were sharply changed (Fig. 3C), which might reveal the L-amino acids may be also participated in biofilm formation induced by UTI89[11] while D-amino acids were catalyzed as dispensable nutrition for bacteria growth[12,13]. In addition, we also noticed that the level changes of different amino acids were extremely distinct between biofilm and planktonic cells. This unregularly phenomenon supported again that amino acids may specially play their individual roles in biofilm formation[14]. Metabolic reprogramming of amino acids in this study was confirmed again to mostly trigger biofilm formation.

AI-2 is a typically quorum-sensing (QS) molecule, it can regulate physiological process of biofilm formation as the density of bacterial cells changed[6]. The lsr protein is essential for importing and processing AI-2, which was noticed to be inhibited by high concentration of Glycerol-3-phosphate (G-3-P)[15]. We speculated that biofilm formation preferred to consume glycerol to biosynthesize G-3-P as it could regulate the expression of AI-2 to avoid biofilm dispersal. This was agreeable with our result that the level of glycerol during biofilm formation was decreased remarkably while the production of G-3-P was enhanced substantially (Fig. 3B). Moreover, the most carbohydrates were incorporated into FimH adhesion (mannose) to increase the adhesive capability of biofilm[16] or participate in the EPS formation. So bacteria would seek other nutrients to maintain their survival. The G-3-P was the key precursor of glyceraldehyde-3-phosphate, it was a key factor that connected the carbohydrate metabolism to glycerolipid metabolism, as well as was a candidate for providing the microbes with the necessary energy. Thus, our finding convinced that more G-3-P has been synthesized, via consuming more glycerol to maintain the survival of bacterial cells during biofilm formation.

Interestingly, our data showed that putrescine was expressed differentially between two modes of UTI89. This result was well supported by previous studies that putrescine plays a crucial role in modulating the biofilm formation triggered by some bacteria[7,17–19]. Another polyamine spermidine was observed to have a remarkable shift in

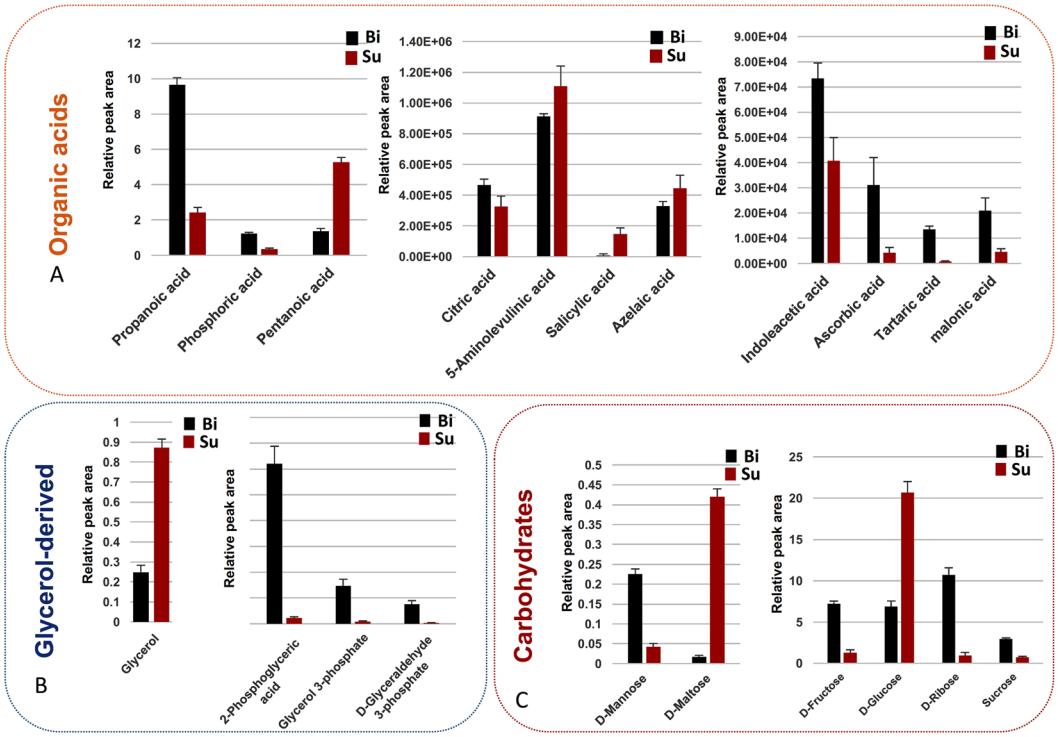

Figure 3. Identifies and their level changes of differential metabolites underlying metabolic reprogramming during biofilm formation while compared to planktonic population. Those differential metabolites mainly include organic acids (**A**), glycerol-derived molecules (**B**), and carbohydrates (**C**). SU: planktonic cells; Bi: Biofilm.

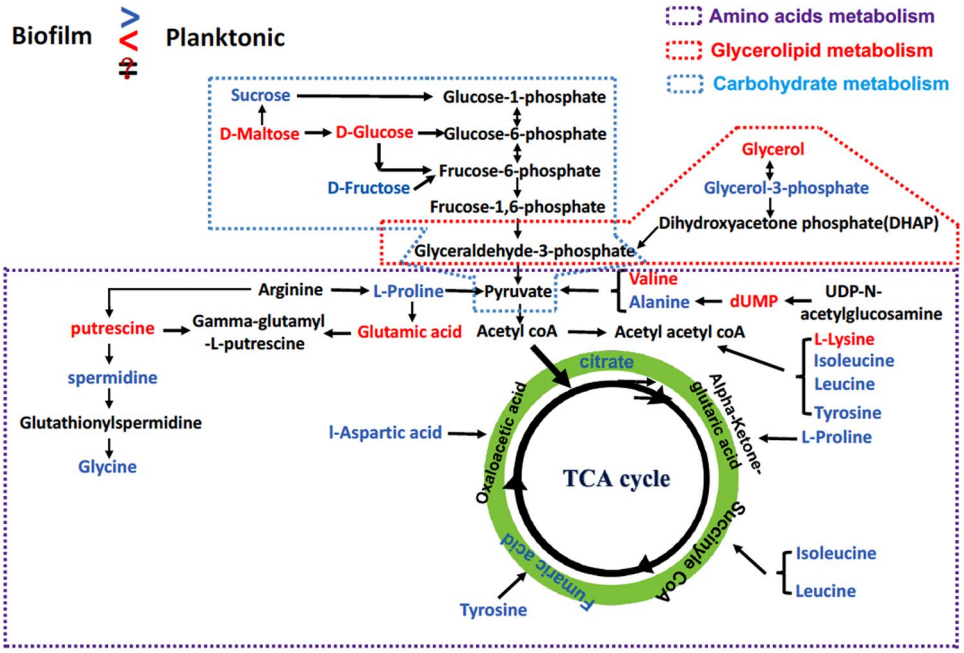

Figure 4. The mostly affected metabolic pathways triggered substantially metabolic reprogramming that permitted biofilm formation induced by UTI89 strain. Amino acid metabolism, glycerolipid and TCA cycle are mostly affected during biofilm formation as differential metabolites in blue were significantly increased in biofilm formation, and blue ones were lowered remarkably.

biofilm formation, which was not expected since spermidine was verified only to inhibit the growth of *E. coli* at PH 7, but not link to the biofilm formation[20]. In near future, we shall figure out to study further the mechanisms of this metabolite modulating biofilm formation.

Bacterial cells in biofilm mode have extraordinary survival ability[21] to resist the environmental stress largely via the protective EPS. Amino acid metabolism, carbohydras metabolism and glycolipid metabolism in bacteria were not only responsible for the biosynthesis and storage of accessible energy but also were utilized for synthesizing the secreted components such as amino acids, sugars, lipids, uridines and organic acids, which are essential for EPS production during biofilm formation[22]. Those metabolic pathways were highlighted in this study to have significantly metabolic reprogramming that triggered the biofilm formation from metabolic perspective (Fig. 4). Those findings indicated that biofilm formation is ought to yield a protective feature, by funneling metabolites into EPS synthesis, conveying the stronger protection against stress conditions via dominating the metabolic reprogramming. Biofilm network is supposed to build a anaerobic microenvironment for bacteria embedded in biofilm pellicle[23], where bacterial cells were structured in a stable space. Thus, bacterial biofilm could secure more resources in order to survive well while compared to planktonic cells.

Conclusion

In summary, this study was first to combine metabolomics with cytology methods together to better understand the biofilm formation in UTI89 strain.

Our data has revealed that obviously metabolic reprogramming triggered biofilm formation while compared to planktonic population as we found lots of small-molecule metabolites are critically essential for biofilm formation and dissociation induced by UTI89. Those differential metabolites and the associated metabolic pathways can be regarded as novel targets for the development of biofilm based treatments and antibiotic discovery against the UTI89 causing infection. More importantly, such effort could provide a novel insight into better understanding of the biofilm formation caused by different bacterial strains at metabolic level.

References

1. Hung, C. *et al*. *Escherichia coli* biofilms have an organized and complex extracellular matrix structure. *mBio* **4**, e00645–00613, https://doi.org/10.1128/mBio.00645-13 (2013).
2. Costerton, J. W., Lewandowski, Z., Caldwell, D. E., Korber, D. R. & Lappin-Scott, H. M. Microbial biofilms. *Annual review of microbiology* **49**, 711–745, https://doi.org/10.1146/annurev.mi.49.100195.003431 (1995).
3. Lv, H., Hung, C. S. & Henderson, J. P. Metabolomic analysis of siderophore cheater mutants reveals metabolic costs of expression in uropathogenic *Escherichia coli*. *Journal of proteome research* **13**, 1397–1404, https://doi.org/10.1021/pr4009749 (2014).
4. Yan, L., Nie, W. & Lv, H. Metabolic phenotyping of the Yersinia high-pathogenicity island that regulates central carbon metabolism. *The Analyst* **140**, 3356–3361, https://doi.org/10.1039/c4an02223h (2015).
5. Hung, C. S. & Henderson, J. P. Emerging concepts of biofilms in infectious diseases. *Missouri medicine* **106**, 292–296 (2009).
6. Kendall, M. M. & Sperandio, V. Cell-to-Cell Signaling in *Escherichia coli* and Salmonella. *EcoSal Plus* **6**, https://doi.org/10.1128/ecosalplus.ESP-0002-2013 (2014).
7. Hobley, L. *et al*. Norspermidine is not a self-produced trigger for biofilm disassembly. *Cell* **156**, 844–854, https://doi.org/10.1016/j.cell.2014.01.012 (2014).
8. Bernier, S. P., Ha, D. G., Khan, W., Merritt, J. H. & O'Toole, G. A. Modulation of Pseudomonas aeruginosa surface-associated group behaviors by individual amino acids through c-di-GMP signaling. *Research in microbiology* **162**, 680–688, https://doi.org/10.1016/j.resmic.2011.04.014 (2011).
9. Valle, J. *et al*. The amino acid valine is secreted in continuous-flow bacterial biofilms. *Journal of bacteriology* **190**, 264–274, https://doi.org/10.1128/JB.01405-07 (2008).
10. Kolodkin-Gal, I. *et al*. D-amino acids trigger biofilm disassembly. *Science (New York, N.Y.)* **328**, 627–629, https://doi.org/10.1126/science.1188628 (2010).
11. Leiman, S. A. *et al*. D-amino acids indirectly inhibit biofilm formation in Bacillus subtilis by interfering with protein synthesis. *Journal of bacteriology* **195**, 5391–5395, https://doi.org/10.1128/jb.00975-13 (2013).
12. Fernandez, M. & Zuniga, M. Amino acid catabolic pathways of lactic acid bacteria. *Critical reviews in microbiology* **32**, 155–183, https://doi.org/10.1080/10408410600880643 (2006).
13. Bayne, H. G. & Stokes, J. L. Amino acid metabolism of Salmonellae. *Journal of bacteriology* **81**, 126–129 (1961).
14. Wong, H. S., Maker, G. L., Trengove, R. D. & O'Handley, R. M. Gas chromatography-mass spectrometry-based metabolite profiling of Salmonella enterica serovar Typhimurium differentiates between biofilm and planktonic phenotypes. *Applied and environmental microbiology* **81**, 2660–2666, https://doi.org/10.1128/AEM.03658-14 (2015).
15. Willias, S. P., Chauhan, S. & Motin, V. L. Functional characterization of Yersinia pestis aerobic glycerol metabolism. *Microbial pathogenesis* **76**, 33–43, https://doi.org/10.1016/j.micpath.2014.08.010 (2014).
16. Schwartz, D. J. *et al*. Positively selected FimH residues enhance virulence during urinary tract infection by altering FimH conformation. *Proceedings of the National Academy of Sciences of the United States of America* **110**, 15530–15537, https://doi.org/10.1073/pnas.1315203110 (2013).
17. Goytia, M., Dhulipala, V. L. & Shafer, W. M. Spermine impairs biofilm formation byNeisseria gonorrhoeae. *FEMS Microbiology Letters* **343**, 64–69, https://doi.org/10.1111/1574-6968.12130 (2013).
18. Burrell, M., Hanfrey, C. C., Murray, E. J., Stanley-Wall, N. R. & Michael, A. J. Evolution and multiplicity of arginine decarboxylases in polyamine biosynthesis and essential role in Bacillus subtilis biofilm formation. *The Journal of biological chemistry* **285**, 39224–39238, https://doi.org/10.1074/jbc.M110.163154 (2010).
19. Wortham, B. W., Oliveira, M. A., Fetherston, J. D. & Perry, R. D. Polyamines are required for the expression of key Hms proteins important for Yersinia pestis biofilm formation. *Environ Microbiol* **12**, 2034–2047, https://doi.org/10.1111/j.1462-2920.2010.02219.x (2010).
20. Nesse, L. L., Berg, K. & Vestby, L. K. Effects of norspermidine and spermidine on biofilm formation by potentially pathogenic *Escherichia coli* and Salmonella enterica wild-type strains. *Applied and environmental microbiology* **81**, 2226–2232, https://doi.org/10.1128/aem.03518-14 (2015).
21. Chauret, C. Survival and control of *Escherichia coli* O157:H7 in foods, beverages, soil and water. *Virulence* **2**, 593–601, https://doi.org/10.4161/viru.2.6.18423 (2011).
22. Larsen, F. H. & Engelsen, S. B. Insight into the Functionality of Microbial Exopolysaccharides by NMR Spectroscopy and Molecular Modeling. *Frontiers in microbiology* **6**, 1374, https://doi.org/10.3389/fmicb.2015.01374 (2015).
23. Hamilton, W. Biofilms: Microbial interactions and metabolic activities. Biofilms: Microbial interactions and metabolic activities. p 361–385 In Hamilton W. A., editor. (ed.), Ecology of microbial communities. University Press, Cambridge, United Kingdom (1987).

Acknowledgements

This work was supported by the National Natural Science Foundation of China Grants (Nos 81274175 and 31670031), National Key R&D Program of China (Nos 2017YFC1308600 and 2017YFC1308605), and the Startup Funding for Specialized Professorship Provided by Shanghai Jiao Tong University (No. WF220441502).

Author Contributions

H.T.L. and Y.M.Q. designed and conceived the experiments; Y.M.Q., X.W., T.B.G., H.G. and H.T.L. collected and analyzed the data; H.T.L. and Y.M.Q. wrote the manuscript. All authors reviewed the manuscript.

Additional Information

Supplementary information accompanies this paper at https://doi.org/10.1038/s41598-019-49603-1.

Competing Interests: The authors declare no competing interests.

Publisher's note: Springer Nature remains neutral with regard to jurisdictional claims in published maps and institutional affiliations.